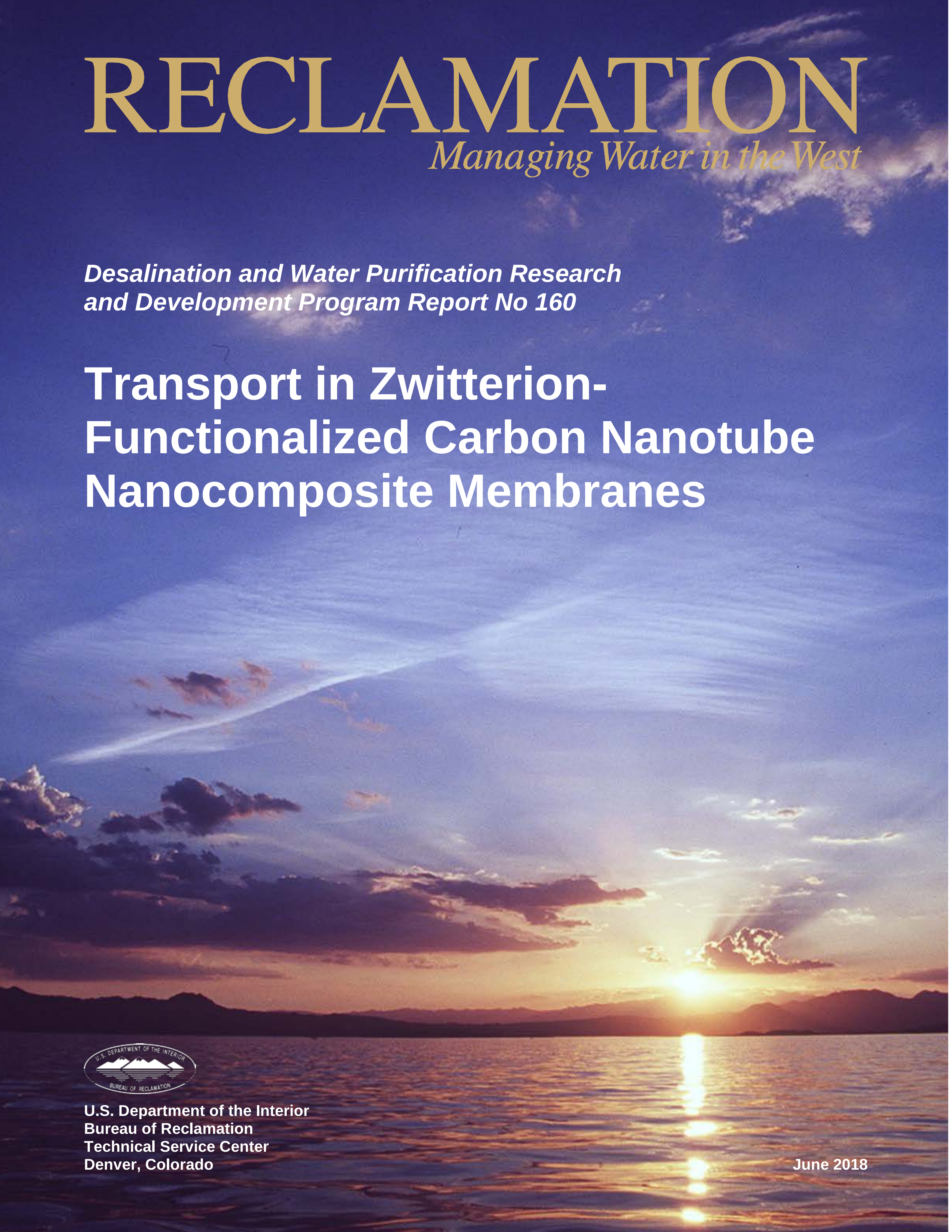

RECLAMATION

Managing Water in the West

Desalination and Water Purification Research and Development Program Report No 160

Transport in Zwitterion-Functionalized Carbon Nanotube Nanocomposite Membranes

U.S. Department of the Interior
Bureau of Reclamation
Technical Service Center
Denver, Colorado

June 2018

REPORT DOCUMENTATION PAGE

Form Approved
OMB No. 0704-0188

1. REPORT DATE *(DD-MM-YYYY)* January 2013	**2. REPORT TYPE** Final	**3. DATES COVERED** *(From - To)* September 2011 to January 2013

4. TITLE AND SUBTITLE Transport in Zwitterion-Functionalized Carbon Nanotube Nanocomposite Membranes	**5a. CONTRACT NUMBER** Agreement No R10AP81214
	5b. GRANT NUMBER
	5c. PROGRAM ELEMENT NUMBER
6. AUTHOR(S) Anil Surapathi, Wai Fong Chen and Eva Marand	**5d. PROJECT NUMBER**
	5e. TASK NUMBER Task III
	5f. WORK UNIT NUMBER
7. PERFORMING ORGANIZATION NAME(S) AND ADDRESS(ES) Department of Chemical Engineering, Virginia Polytechnic Institute and State University, 138 Randolph Hall, Blacksburg, VA 24061	**8. PERFORMING ORGANIZATION REPORT NUMBER**
9. SPONSORING/MONITORING AGENCY NAME(S) AND ADDRESS(ES) Bureau of Reclamation U.S. Department of the Interior Denver Federal Center PO Box 25007, Denver, CO 80225-0007	**10. SPONSOR/MONITOR'S ACRONYM(S)** Reclamation
	11. SPONSOR/MONITOR'S REPORT NUMBER(S) DWPR Report No. 160

12. DISTRIBUTION/AVAILABILITY STATEMENT
Online at https://www.usbr.gov/research/dwpr/DWPR_Reports.html

13. SUPPLEMENTARY NOTES

14. ABSTRACT

The primary goal of our project was to fabricate and characterize the desalination performance of zwitterion-functionalized carbon nanotube membranes. Using a patented fabrication method, developed in our laboratory, we have made CNT membranes consisting of dense, vertically oriented carbon nanotubes on a porous support. The advantage of this approach is that the carbon nanotubes can be obtained commercially or synthesized specifically for a given application with the desired pore size and functionality. The zwitterion functionalized CNT membranes demonstrated extremely high transport rates, both for gas as well as water.

15. SUBJECT TERMS
Carbon nanotube, membranes, desalination, zwitterion

16. SECURITY CLASSIFICATION OF:			**17. LIMITATION OF ABSTRACT**	**18. NUMBER OF PAGES**	**19a. NAME OF RESPONSIBLE PERSON** Yuliana Porras-Mendoza
a. REPORT U	**b. ABSTRACT** U	**a. THIS PAGE** U	SAR		**19b. TELEPHONE NUMBER** *(Include area code)* 303-445-2265

Standard Form 298 (Rev. 8/98)
Prescribed by ANSI Std. Z39.18

Desalination and Water Purification Research
and Development Program Report No. 160

Transport in Zwitterion-Functionalized Carbon Nanotube Nanocomposite Membranes

Prepared for Reclamation under Agreement No. R10AP81214

by

Anil Surapathi, Wai Fong Chen and Eva Marand

for

Virginia Polytechnic Institute and State University

Mission Statements

The U.S. Department of the Interior protects America’s natural resources and heritage, honors our cultures and tribal communities, and supplies the energy to power our future.

The mission of the Bureau of Reclamation is to manage, develop, and protect water and related resources in an environmentally and economically sound manner in the interest of the American public.

Disclaimer

Acknowledgments

The Desalination and Water Purification Research and Development Program, Bureau of Reclamation, is the sponsor of the research.

Acronyms and Abbreviations

Cd^{2+}	cadmium ion
CH_4	methane
CNT	carbon nanotube
CO_2	carbon dioxide
COOH	carboxyl
Cu^{2+}	copper ion
H_2	hydrogen
He	helium
IGA	intelligent gravimetric analyzer
MPD	m- phenylenediamine
MV^{2+}	methyl viologen
N_2	nitrogen
Ni^{2+}	nickel ion
nm	nanometer
O_2	oxygen
OH	hydroxyl
Pb^{2+}	lead ion
PES	polyethersulfone
$Ru\text{-}(bipy)_3^{+2}$	ruthenium bipyridine
SEM	scanning electron microscopy
SF_6	sulfur hexafluoride
TFN	thin film nanocomposite
TGA	thermogravimetric analysis
THF	tetrahydrofuran
TMC	trimesoyl chloride
Zn^{2+}	zinc ion

Measurements

%	percent
°C	degrees Celsius
µm	micrometer
Å	Angstrom
bar	100,000 Pascals
GFD	gallons per square foot per day
mbar	millibar
mg	milligram
mL	milliliter
mmol	millimole
mmol/g	millimole per gram
psi	pounds per square inch
w/v	weight/volume

Contents

Page

Mission Statements iv
Disclaimer iv
Acknowledgments iv
Acronyms and Abbreviations iii
Measurements iii
1. Introduction 1
    1.1. Background 1
    1.2. Goals and Objectives 2
2. Experiments 3
    2.1. Materials 3
    2.2. Fabrication of Polyamide/SWNT Nanocomposite Membranes 5
        2.2.1. Dispersion of SWNTs and Alignment by High Pressure Filtration 5
        2.2.2. Interfacial Polymerization 5
    2.3. Characterization 6
3. Results and Discussion 7
    3.1. SEM 7
    3.2. TGA 7
    3.3. Gas Sorption Isotherms 8
    3.4. Gas Transport Properties of Functionalized SWNT/Polyamide Nanocomposite Membranes 11
    3.5. Desalination Results 15
        3.5.1. Performance as a Function of CNTs' Concentration 15
        3.5.2. Performance as a Function of Hydraulic Pressure 16
4. Conclusions 17
5. References 18

Figures

Page

1 Schematic of the chemical reactions leading to the formation of zwitterion groups on the carbon nanotube tips 3
2 Four zwitterionic functional groups at the carbon nanotube tip 4
3 Cross section SEM image of functionalized SWNT/polyamide membrane 7
4 Thermogravimetric plot of COOH and zwitterion functionalized SWNTs 8
5 Sorption isotherms of COOH functionalized SWNTs at 350 °C 10
6 Sorption isotherms in zwitterion functionalized SWNTs at 35 °C 10
7 CO_2 gas sorption in COOH, zwitterion functionalized (heated to 200 °C) and zwitterion functionalized (not heated) SWNTs 11

8 Gas permeabilities of different gases in zwitterion functionalized SWNT polyamide nanocomposite membrane 12
9 Selectivities of gases with respect to He in different nanocomposite membranes 13
10 Permeability of various light gases through 1 mg SWNT TFN membranes with different functionalizations (zwitterion and carboxylic acid groups) 14
11 Selectivities of various light gases through 1 mg SWNT TFN membranes with different functionalizations (zwitterion and carboxylic acid groups) 14
12 Water flux and salt rejection (%) as a function of CNT content 15
13 Water flux and salt rejection as a function of pressure 16

Tables

page

1 Comparison of Different Nanocomposite Membranes with Increasing Zwitterion-Functionalized CNT Density 15
2 Plain PA (March 22, 2012) 16
3 0.25 mg-CNT + 0.5 %TMC-PA (March 16, 2012) 17
4 0.75 mg CNT + 0.5%TMC-PA (March 26, 2012) 17
5 Reverse Osmosis for 1,000 Parts Per Million Magnesium Sulfate Solution 17

1. Introduction

1.1. Background

Carbon nanotubes (CNTs) have long been of technical interest due to their exceptional electrical, thermal, and mechanical properties. More recently, molecular simulations and experimental studies have led to the discovery of unique transport properties of fluids within CNTs due to the unprecedented smoothness and regularity of the CNT pores.[2-5,7,26,27] These studies suggest that the transport of water through subnanometer CNTs occurs via a cooperative, pulse-like movement of hydrogen-bonded molecules within the channel, similar to that observed in aquaporin biological channels.[28] This transport mechanism has been shown to lead to more rapid flow rates than those predicted by classical hydrodynamics.[29,30] The observed enhanced water transport, together with CNT pore diameters on the order of nanometers, presents the possibility of employing CNTs to filter ions from water.

To date, there have been very few fundamental studies of transport of small ions through single-walled CNTs. Recent molecular dynamics simulation studies[31,32] have examined the ability of CNTs with diameters ranging from 6 to 11 Angstrom (Å) to filter ions from water. These results indicated that ions can be almost completely excluded from pores up to 9 Å in diameter due to ion desolvation energy barriers. By contrast, water faces relatively low energy barriers and is able to pass through these small nanotubes, but at much lower rates than in larger nanotubes. The work did not address the effects of charged functionalities in the CNT open tips on ion transport. Also using molecular simulation, Joseph and Aluru (2008)[33] explored the occupancy of ions in CNT channels when partial charges were placed on the rim atoms of the nanotubes, and an external field was applied along their axis. As shown in the simulation results, the ion occupancy in a carbon nanotube solvated in an electrolyte was very low for neutral nanotubes and increased significantly in the presence of charged functionalities.

Experimental work on ionic flux through functionalized CNTs has been performed by Hinds et al. (2004).[34] Their work has focused on studying transport of two different sized, but equally charged, molecules: ruthenium bipyridine [Ru-(bipy)$_3^{+2}$] and methyl viologen [MV^{2+}], through multiwalled CNTs with 7-nanometer (nm) nominal core diameters. The effective pore size of the CNT was adjusted by introducing functional groups at the ends of the nanotubes. They examined molecules such as straight chain alkanes, anionically charged dye molecules, and aliphatic amines elongated by polypeptide spacers at the CNT tips. In general, functionalizing the membrane with anionically charged dye molecules increased flux of the positively charged species. This effect was reduced at higher solution ionic strength consistent with shorter Debye screening length. Rao et al.

(1997)[35] have examined the sorption of divalent metal ions, such as lead (Pb^{2+}), nickel (Ni^{2+}), zinc (Zn^{2+}), cadmium (Cd^{2+}), and copper (Cu^{2+}), from aqueous solution onto different carbon nanotube materials such as raw and surface oxidized multi-walled and single-walled CNTs. Sorption of the ions, however, occurred only on the surface of the nanotubes (especially those with many defects, which provided carboxylic acid sorption sites), not in the CNT core. The sorption of the divalent metal ions reached a maximum at a pH range of 8-11, while 90-percent (%) desorption was achieved at a pH of 1.

Zwitterion functionalized surfaces show anti-biofouling features that are of interest in membrane applications because biofouling constitutes a serious problem in desalination applications. In this study, we aimed to synthesize efficient ion selective membranes that do not face biofouling issues. We also hypothesized that zwitterions can enhance the selectivity of the functionalized nanotubes for water over ions. Hence, the focus on zwitterionic functional groups is a way to achieve multidimensional objectives. To the best of our knowledge, no systematic study exists to reveal the effect of functionalization of nanotubes on the transport of ions and water through CNTs. Won et al. (2006)[36] have shown from simulations that charge distributions on free standing CNTs affect the free energy of ions and water inside the CNT. This report indicates the possibility of significant thermodynamic effects due to the functionalization of nanotubes. We note here that the reported charge distributions by Won et al. may not be physical because, in reality, the tips of CNTs are functionalized with various groups such as carboxyl (COOH), hydroxyl (OH), etc., which arise from the oxidation of the caps routinely used to open the CNTs. Suk and Aluru (2009)[37] have shown that applying electric fields to nanotubes affects the flux of water under applied pressure for (6,6) CNTs; therefore, different zwitterion functional groups on the entrance of CNTs can be an important design tool. Studies on (10,10) boron nitride nanotubes versus (10,10) CNTs[38] show reversed selectivity of K^+ and Cl^- ions due to different entrance effects that result from the difference in charges at the entrance of the nanotubes. All of these results indicate that tip entrance and charge effects are key to the design of high-efficiency, functionalized nanotube membranes.

1.2. Goals and Objectives

The primary goal of our project was to fabricate and characterize the desalination performance of zwitterion-functionalized carbon nanotube membranes. Using a patented fabrication method developed in our laboratory12, we have made CNT membranes consisting of dense, vertically oriented carbon nanotubes on a porous support. The advantage of this approach is that the carbon nanotubes can be obtained commercially or synthesized specifically for a given application with the desired pore size and functionality. Furthermore, the CNTs can be purified, and their pore size and pore-size distribution can be characterized before they are assembled into a CNT membrane. In this study, we have employed porous polymeric supports and interfacial polymerization to fix the carbon nanotubes in a polymer matrix, an approach that should be easily adaptable in commercial membrane fabrication involving large surface areas.

The transport data reflect three separate characterization efforts: gas sorption measurements, gas transport measurements, and water flux and salt rejection measurements.

2. Experiments

2.1. Materials

COOH functionalized single-walled nanotubes (SWNTs) with an outer diameter of 1.5 nm and a length of 1 microgram (µm) were purchased from Nano Lab, Inc., in Massachusetts. The CNTs were produced by a chemical vapor deposition method, purified and functionalized with COOH groups by refluxing in sulfuric acid/nitric acid. Purity of the SWNTs was greater than 95 % (by thermogravimetric analysis (TGA). Concentration of COOH groups in the SWNTs was approximately 2-7% by weight (by titration). Polyethersulfone (PES) microporous supports were purchased from Trisep Corp., in California. The two reagents, m- phenylenediamine (MPD) (≥99% purity) and trimesoyl chloride (TMC) (98% purity were purchased from Sigma-Aldrich and used without any additional purification. Hexane (99.9% purity) was purchased from Fischer Scientific. Surfactant, sodium dodecylbenzene sulfonate (80% purity) was purchased from Sigma.

Figure 1 describes the synthesis of the zwitterionic functionalized SWNTs. The zwitterion functional group is circled in red. The COOH groups on the SWNTs served as precursors for the addition of zwitterion groups.

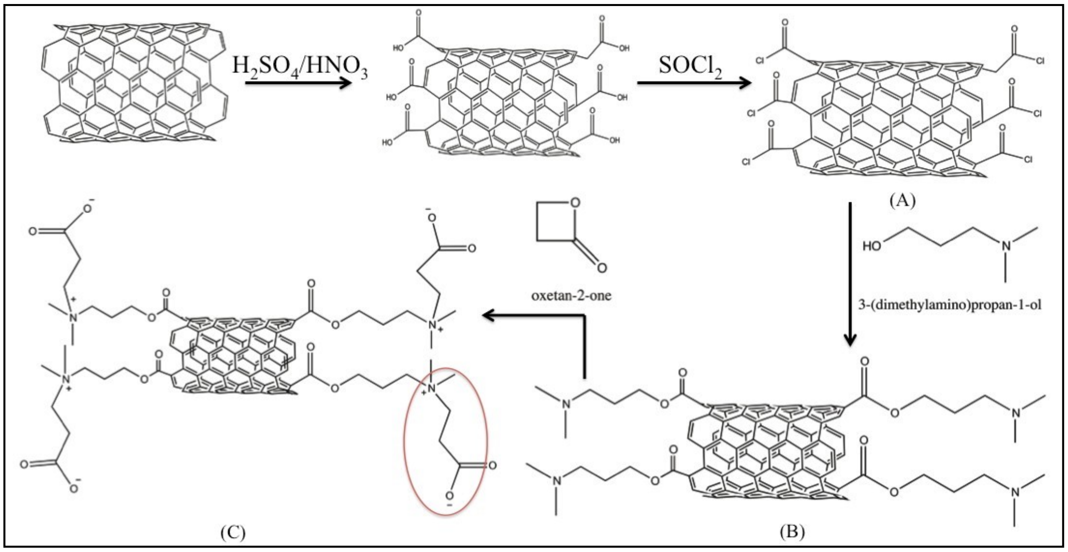

Figure 1.—Schematic of the chemical reactions leading to the formation of zwitterion groups on the carbon nanotube tips.

In the first step, COOH functionalized SWNTs were reacted with thionyl chloride to form COCl groups (figure 1(A)). The acyl chloride functionalized SWNTs were reacted with 3-(dimethylamino)propan-1-ol to form the compound shown in figure 1(B). In brief, 100 milligrams (mg) of COCl SWNTs (0.1 millimole (mmol) of COCl group) were added to a mixture of 1.2 milliliters (mL) 3-(dimethylamino)propan-1-ol (10 mmol) and 1.4 mL of triethyl amine (10 mmol) in a 100-mL flask. The reaction mixture was stirred for 6 days at 100 revolutions per minute at room temperature. In the second step, the SWNTs were then washed with ethanol to remove ethylamine hydrochloride salt and were dried under vacuum. In the third step, SWNTs were reacted with β-propiolactone to form zwitterion functionalized SWNTs. 100 mg of (B) functionalized SWNTs were added to 20 mL of dry tetrahydrofuran (THF) in a 50-mL flask. The reaction mixture was stirred under nitrogen protection at room temperature for 5 hours. SWNTs were washed with dry THF and separated by centrifuging. They were dried under vacuum to remove any washing solvent. Figure 2 shows a molecular perspective of the functionalized carbon nanotube. The maximum number of zwitterionic groups that can fit around a carbon nanotube tip of ~15 Å diameter is four.

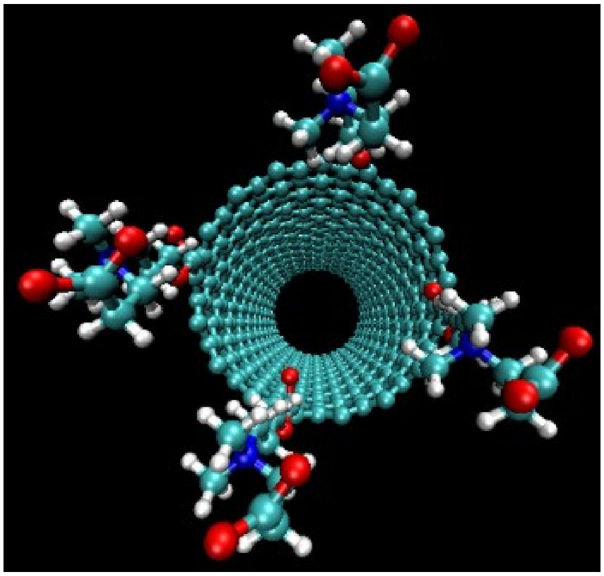

Figure 2.—Four zwitterionic functional groups at the carbon nanotube tip (courtesy of Professor Karl Johnson, University of Pittsburgh, all rights reserved).

2.2. Fabrication of Polyamide/SWNT Nanocomposite Membranes

2.2.1. Dispersion of SWNTs and Alignment by High Pressure Filtration

A predetermined amount of zwitterion functionalized SWNTs was sonicated in deionized water. The PES membrane support was pretreated by soaking in a 0.5% weight/volume (w/v) surfactant solution of sodium dodecyl benzene sulfonate for 2 days. This pretreatment was necessary to make the membrane support more hydrophilic.

The aqueous SWNT suspension was then deposited on the membrane support using a high-vacuum filtration method, in which the support acted as a filter paper and the CNTs were filtered out of the solution and aligned on the support. The high-pressure filtration was assumed to align the SWNTs in the direction of the flow of the solvent. The filter disc, with a thin layer of SWNTs, was dried under vacuum for 12 hours. The SWNTs alignment was locked by polyamide matrix polymer, formed by interfacial polymerization as discussed below. The concentration of the SWNTs in the polymer matrix ranged from 0% to approximately 40% by weight. Table 1 summaries the various samples and their concentrations.

Table 1. Weight Concentrations of Functionalized SWNTs in Matrix Polymer

Weight of Zwitterion –SWNTs (mg)	Weight % of Z-SWNTs in polyamide layer
0	0
1	13
1.5	19
2	24
5	43

2.2.2. Interfacial Polymerization

For interfacial polymerization, two solutions containing the monomers were prepared. The aqueous solution consisted of 2% (w/v) MPD in water along with 0.2% (w/v) surfactant to improve the wetting of the support by the solution. The organic solution consisted of TMC 0.5 % (w/v) in hexane.

The PES support with the deposited CNTs was placed between two circular Polytetrafluoroethylene frames that were held together with a metal clamp. The polyester side of the PES support was soaked with MPD for 1 minute. After that, the MPD solution was drained, the support was dried for 1 minute, and the excess MPD solution was cleaned with a Kim wipe. The TMC solution was then introduced on the polysulfone side of the support using a syringe. The TMC solution was drained very slowly after 2 minutes. The reaction time for the interfacial polymerization was 2 minutes. The thin film nanocomposite (TFN) membrane prepared was cured in an air-circulated oven at 68 degrees Celsius (^{o}C) for 5 minutes. The membrane was washed in deionized water to remove excess MPD, and then stored in water for at least 1 day before testing for either gas separation or desalination.

2.3. Characterization

The cross-section morphology of the SWNT/polyamide membranes was analyzed by scanning electron microscopy (SEM) (LEO 1550 field emission scanning electron microscope. Functionalized SWNTs were characterized by TGA and gas and water sorption isotherms. For TGA characterization, approximately 10 mg of sample was placed in a metal pan and heated from room temperature to 700 ^{o}C.

Sorption properties of zwitterion and COOH functionalized SWNTs were studied using intelligent gravimetric analyzer (IGA 002), Hiden Analytical, Inc., in the United Kingdom. Approximately 20 mg of CNT powder was placed in a metal basket, which was placed inside a gas chamber and degassed by applying a high vacuum ($P < 10^{-4}$ millibar [mbar]). The sample was heated to 200 ^{o}C to remove any absorbed/adsorbed water in the sample when appropriate. All sorption data was recorded at 35 ^{o}C over a gas pressure ranging from 0 to 10 bar (0 to 1 million Pascals).

The gas transport properties of the membranes were measured using a constant-volume permeability apparatus. Two types of membranes were studied. One type of membrane was made using COOH-SWNTs, and the other membrane was made with zwitterion- SWNTs. All permeation tests were performed at room temperature with 2 atmospheres feed pressure and vacuum on the permeate side. The gases used in the experiment were hydrogen (H_2), helium (He), oxygen (O_2), nitrogen (N_2), methane (CH_4), carbon dioxide (CO_2), and sulfur hexafluoride (SF_6).

Water flux and salt rejection measurements were carried out using a laboratory-scale, cross-flow membrane test unit comprised of a membrane cell (General Electric’s Sepa^{TM} CF cell), high pressure pump (hydra-cell pump, Wanner Engineering), back-pressure regulator (U.S. Paraplate), bypass valve (Swagelok), feed water reservoir (Nalgene), a closed loop mode where both permeate and retentate are circulated into the feed water reservoir. The salt concentration was measured with a conductivity meter calibrated for salt ions over the concentration range of interest.

3. Results and Discussion

3.1. SEM

Figure 3 shows the SEM image of the cross -section of the zwitterion functionalized SWNT TFN membranes. The porous region in the image represents a PES polyethersulfone layer, which is present on top of the polyester support. The Tthin, dense layer on top of the PES layer is approximately 500 nm thick and consists of the polyamide layer with zwitterion functionalized SWNTs. At this magnification, it is imnot possible to see the SWNTs embedded in the polyamide polymer. Because of the low magnification, we cannot comment on the degree of alignment of the tubes within the matrix polymer by looking at the image.

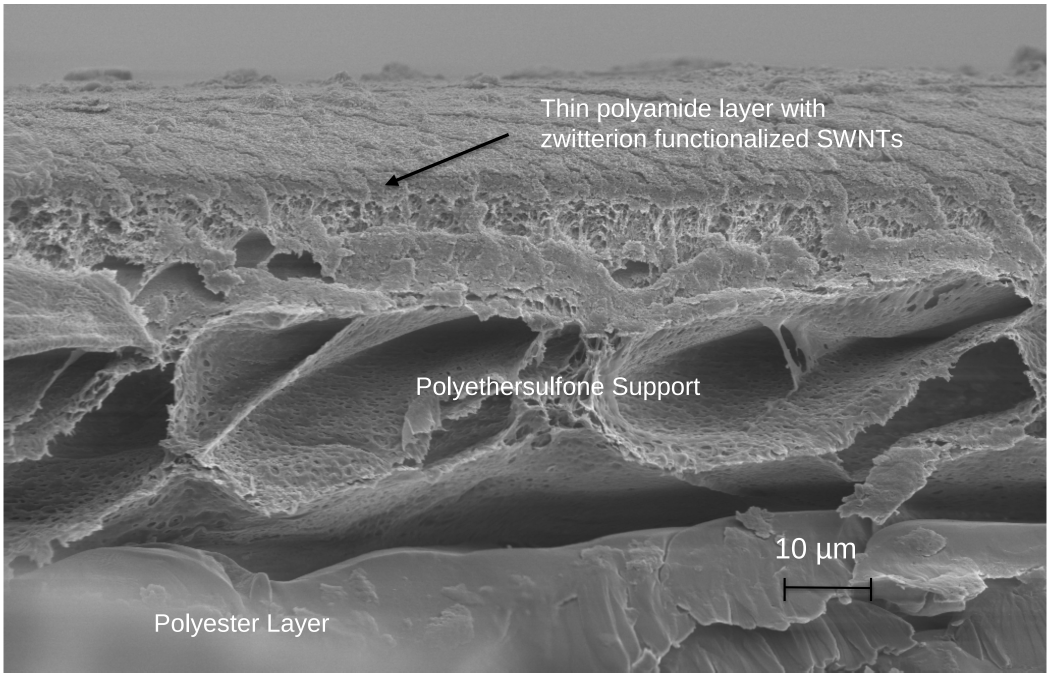

Figure 3.— Cross section SEM image of functionalized SWNT/polyamide membrane.

3.2. TGA

Figure 4 shows TGA weight loss curves corresponding to COOH functionalized and zwitterion functionalized SWNTs. The COOH functionalized carbon nanotubes begin to lose weight around 450 °C (most likely associated with the pyrolysis of organic groups) and reach 0% weight at 650 °C when the remaining carbon structures are pyrolyzed [3, 4, 5]. In the case of zwitterion functionalized carbon nanotubes, the weight loss occurs in stages, starting at 150 °C and then at 450 °C.

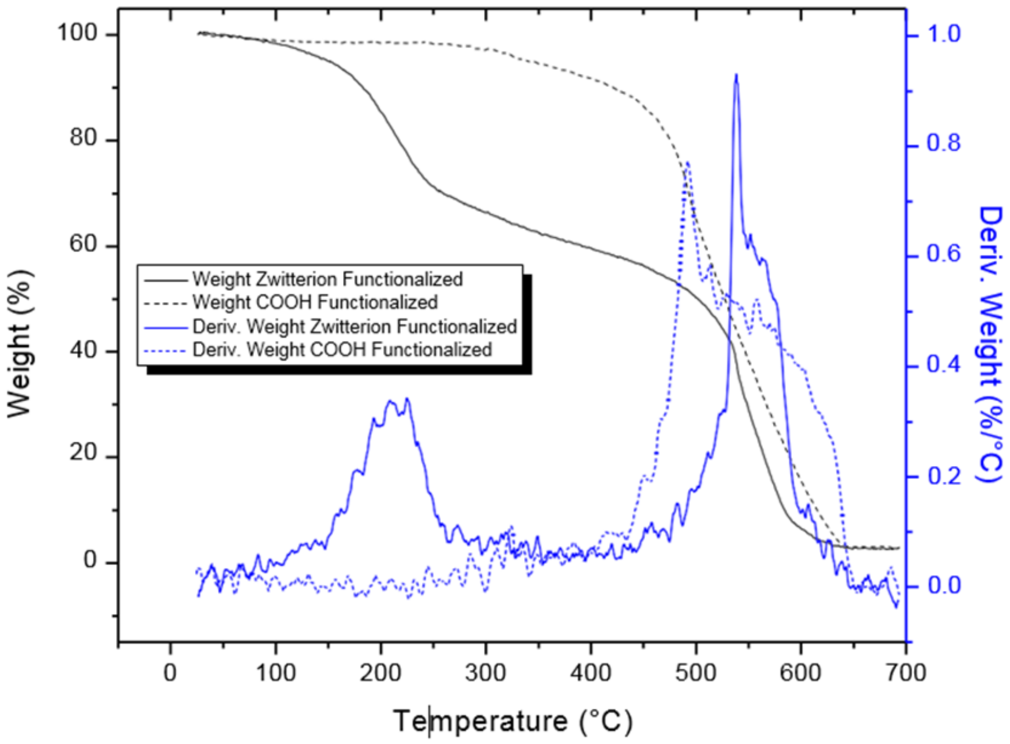

Figure 4.—Thermogravimetric plot of COOH and zwitterion functionalized SWNTs.

To explain this behavior, we look at the weight derivative plot of zwitterion functionalized SWNTs, which has a peak at 200 °C not observed in the COOH functionalized SWNTs. This early weight loss may be attributed to loosely bound water in SWNTs. Zwitterionic functional groups exhibit large affinity to absorb water via electrostatic interactions with water molecules[2, 10].·This water, as we shall demonstrate later, can be removed by heating the sample above 200 °C. The weight derivative plot of the zwitterion SWNT also demonstrates the need for higher temperatures (550 °C) to pyrolyze the organic zwitterionic groups, as opposed to the carboxylic acid groups, which begin to pyrolyze near 450 °C.

3.3. Gas Sorption Isotherms

The approximate size of zwitterion and COOH functional group is around 1.1-1.2 nm and 0.4 nm, respectively; thus, the presence of the groups may affect the effective pore diameter of the SWNTs. The effective pore diameter is defined as the diameter of the largest gas molecule that can enter inside the tube through its opening. This dimension depends on the diameter of the SWNTs, as well as the molecular interactions between the gas molecule and the functional groups present at the entrance of the tube. Sorption isotherm represents the concentration of the gas sorbed in the SWNTs as a function of gas pressure inside the chamber at a given temperature. At each pressure, the equilibrium weight of the sample is recorded and used for calculating the uptake or the concentration of the sorbed gas. The equilibration criterion for advancing to the next isotherm point is satisfied when the uptake has changed by a 0.99 fraction of the difference between the initial reading (at the beginning of the isotherm point) and the predicted asymptote. IGA used the linear driving force model to fit the mass uptake data and predict the asymptotic uptake. The instrument software using the above model parameters predicts the total run time at a particular isotherm point. For certain materials, this run time can be very long, depending on the characteristics of the gas diffusion.

Figure 5 shows sorption isotherms of COOH functionalized SWNTs for gases CO_2, N_2 and CH_4. The amount of gas sorbed increased in the following order: N_2, CH_4, and CO_2; hence, COOH SWNTs are more sorption selective to CO_2 gas ($C = 6.21$ millimoles per gram [mmol/g] at $P = 10$ bar) than CH_4 ($C = 3.17$ mmol/g at $P = 10$ bar), and more sorption selective to CH_4 than N_2 ($C = 1.51$ mmol/g at $P = 10$ bar). Figure 6 shows sorption isotherm of various gases in zwitterion functionalized SWNTs.

On comparing the isotherms of N_2, CH_4, and CO_2 in figures 5 and 6, it can be inferred that a lower amount of gas sorbed in zwitterionic functionalized SWNTs than in COOH functionalized SWNTs. This very low sorption is most likely due to the zwitterion functional groups blocking gas molecules from entering/sorbing inside the nanotube. As mentioned earlier, zwitterionic functional groups are 1.1-1.4 nm in length, which is comparable to the diameter of the SWNT (1.5 nm). Hence, their presence reduces the effective pore diameter to virtually zero. In that case, the small sorption of CO_2 at these conditions may be attributed to surface sorption. On the other hand, the size of the COOH groups (0.4 nm) is not large enough to completely block the opening of the carbon nanotubes. The presence of the COOH groups, however, still affects the sorption of gases in SWNTs, as demonstrated in our previous studies, where the sorption of CO_2 was lowered by half in COOH functionalized SWNTs compared to nonfunctionalized nanotubes. Zwitterion functionalized SWNTs are also sorption selective for CO_2 ($C = 0.31$ mmol/g at $P = 10$ bar) over CH_4 ($C = 0.05$ mmol/g at $P = 10$ bar) and not very significant for CH_4 over N_2 ($C = 0.04$ mmol/g at $P = 10$ bar). However, the absolute value of concentration of CO_2 gas sorbed in zwitterion SWNTs ($C = 0.31$ mmol/g at $P = 10$ bar) is lower than COOH SWNTs ($C = 6.21$ mmol/g at $P = 10$ bar).

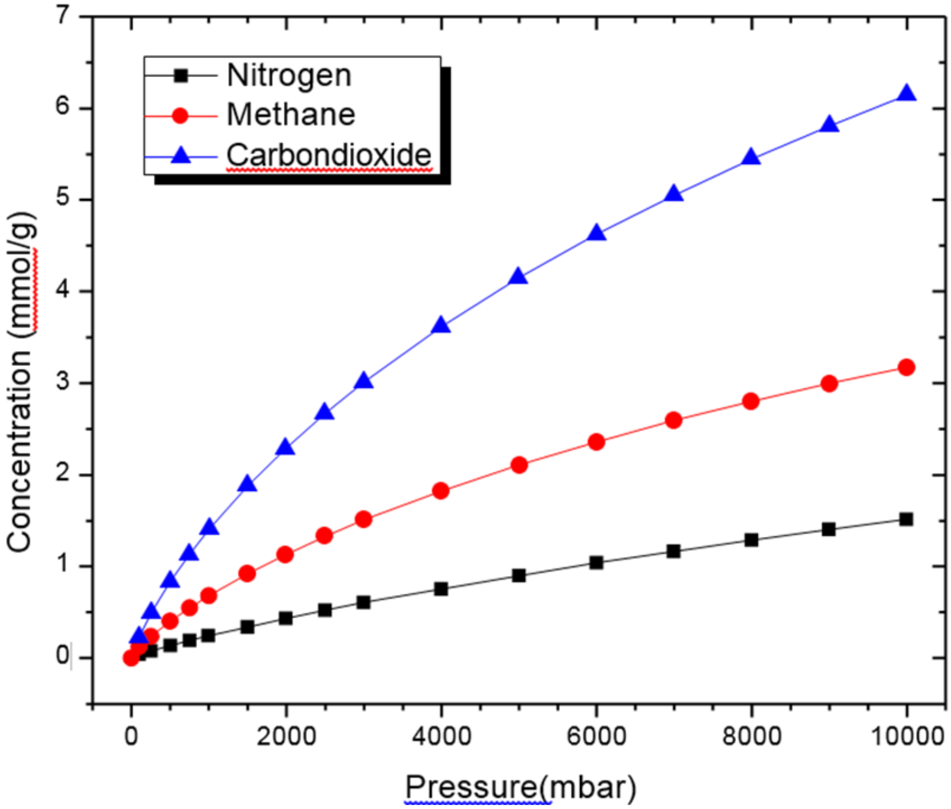

Figure 5.—Sorption isotherms of COOH functionalized SWNTs at 350 °C.

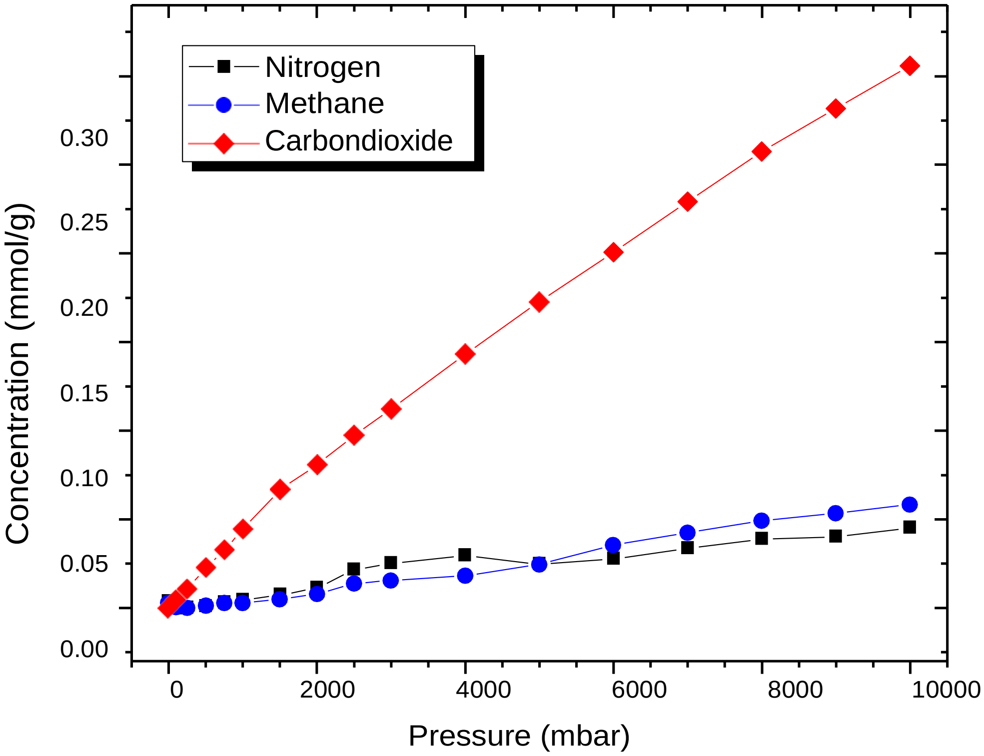

Figure 6.—Sorption isotherms in zwitterion functionalized SWNTs at 35 °C.

Earlier, in the TGA graph of zwitterion functionalized SWNTs, we observed that these SWNTs lose water molecules upon heating to 200 °C. Until now, the zwitterion SWNTs studied in the sorption study were not heated. We hypothesize that the water molecules sorbed in the zwitterion SWNTs decrease gas sorption. To prove this, the zwitterion SWNTs were heated to 200 °C, and the gas sorption isotherms were measured again. As expected, a significant weight loss of the sample was observed after heating, and the concentration of CO_2 gas sorbed increased. Figure 7 shows these results. The concentration of CO_2 gas increased from 0.31 mmol/g (at 10 bar) in hydrated zwitterion SWNTs to 1.7 mmol/g (at 10 bar) in nonhydrated (heated) zwitterion SWNTs. This is a significant increase, reflecting the removal of water molecules blocking the SWNTs pores.

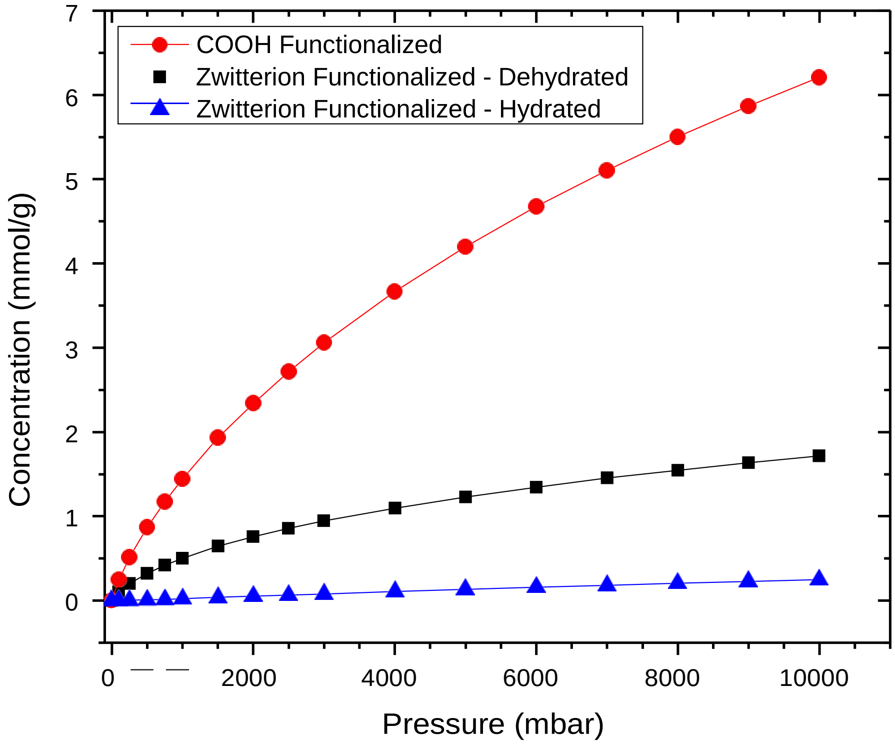

Figure 7.— CO_2 gas sorption in COOH, zwitterion functionalized (heated to 200 °C) and zwitterion functionalized (not heated) SWNTs.

3.4. Gas Transport Properties of Functionalized SWNT/Polyamide Nanocomposite Membranes

Thin film nanocomposite membranes having different SWNT concentrations in the polyamide separation layer were fabricated and tested for their gas transport properties. Table 1 summarizes these concentrations. Figure 8 shows the gas permeabilities of light gases (H_2, He, N_2, O_2, CH_4, CO_2 and SF_6) in the zwitterion functionalized SWNT TFNs in comparison to gas permeabilities in the neat polyamide membrane. As is evident in the plot, the permeabilities of all gases increased with increasing concentration of the CNTs in the separation layer. For example, the H_2 permeability increased by a factor of 25 from 325 Barrer in the pure PA to 8072 Barrer in the 5-mg CNT polyamide membrane. Similar increases are observed for other gases (factor increase in parenthesis): He (19), N_2 (19), O_2 (33), CH_4 (21), CO_2 (37), and SF_6 (29). This tremendous increase in permeability is due to the transport through the CNT pores, as well as through possible nanochannels formed around individual CNTs within CNT bundles. Although this cannot be proven directly, the increase in permeability of each gas with the concentration of CNTs in the matrix would be consistent with this explanation because the number of nano-channels would be expected to increase with CNT content.

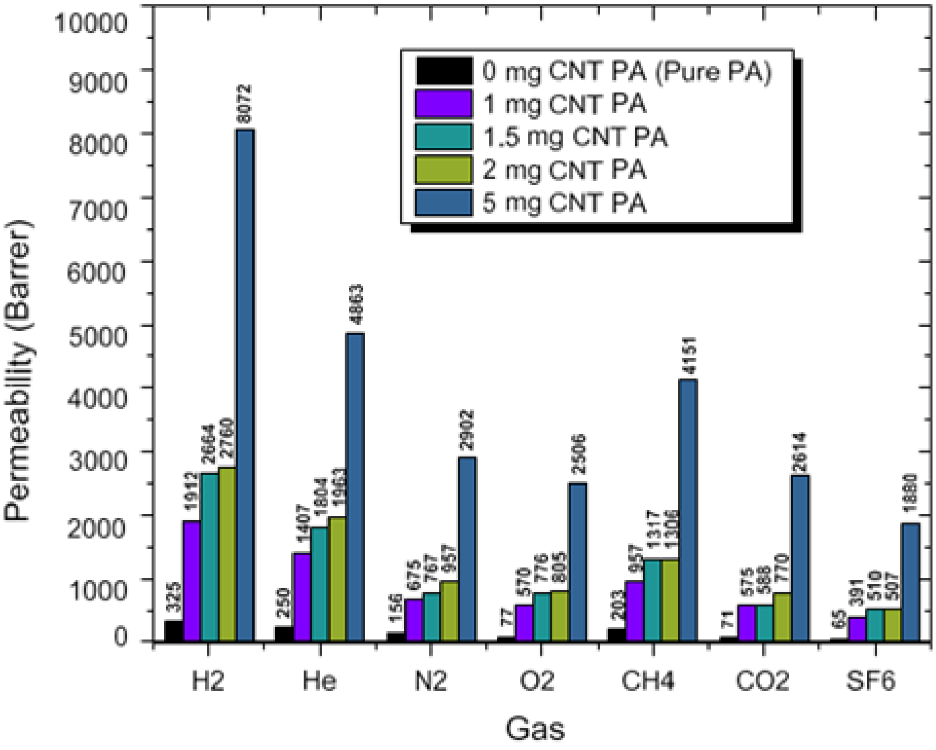

Figure 8.—Gas permeabilities of different gases in zwitterion functionalized SWNT polyamide nanocomposite membrane.

Figure 9 shows the selectivities of various gases with respect to He for TFN membranes with varying concentration of zwitterion functionalized SWNTs. As can be seen from the data, the selectivities of gases with respect to He remain nearly constant across all compositions. Unfortunately, this result does not support the idea that functionalization of the CNTs with these particular zwitterionic groups will improve selectivity; however, the membranes retain the intrinsic selectivity of the polyamide, while having tremendous enhancements in permeability.

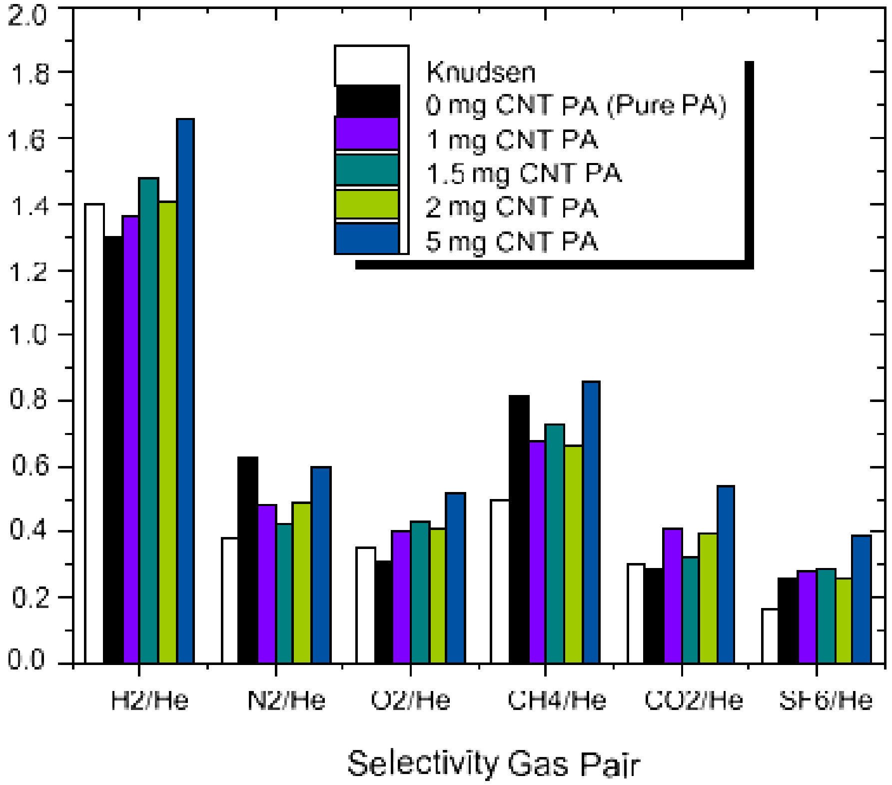

Figure 9.—. Selectivities of gases with respect to He in different nanocomposite membranes.

Figure 10 compares the permeabilities of the two types of membranes at the same CNT composition. Although the gas permeabilities in both types of SWNT membranes are higher than the pure polyamide membrane, the gas permeabilities in the COOH functionalized SWNTs membrane are significantly higher than in the zwitterion functionalized SWNTs membrane. These results are consistent with our previous studies.

Figure 11 compares the selectivities of gases with respect to He in both types of functionalized SWNTs membranes and the neat PA membrane of the same thickness. The selectivities change very little, suggesting that the separation is controlled by the inherent selectivity of the polyamide coating.

The molecular diffusion in these nanostructured membranes clearly takes place through the inner CNT pores, partly through the nanochannels, and eventually through the polymer matrix. Hence, the overall selectivity of the membrane is affected by all three modes of transport. The gas selectivities in the nanostructured membranes, as well as in the neat polyamide membrane, are very similar and very close in value to selectivities predicted by the Knudsen model. The low selectivities in the PA membrane may reflect a loose polymer structure attained during interfacial polymerization.

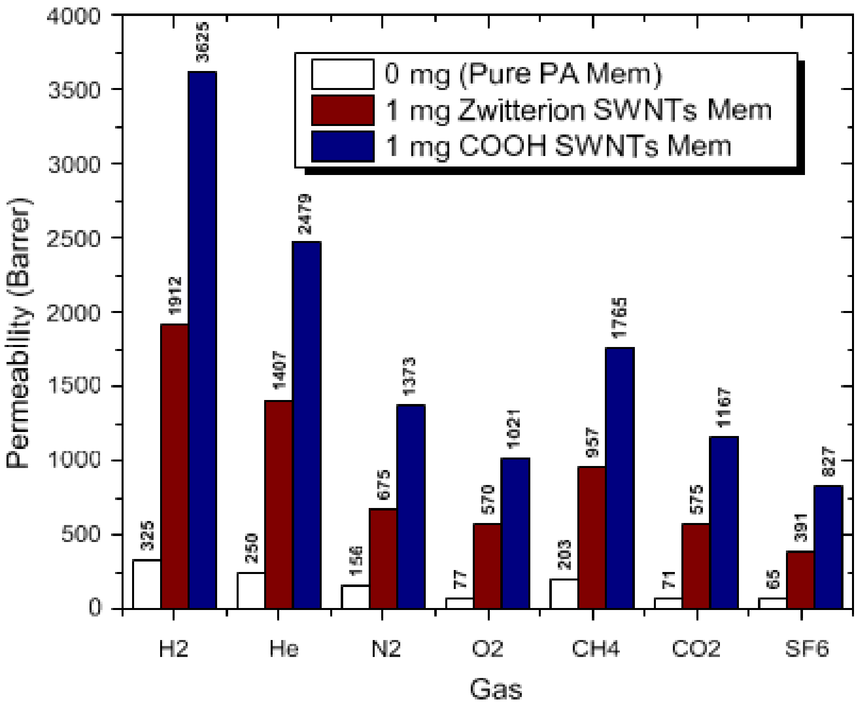

Figure 10.—Permeability of various light gases through 1 mg SWNT TFN membranes with different functionalizations (zwitterion and carboxylic acid groups).

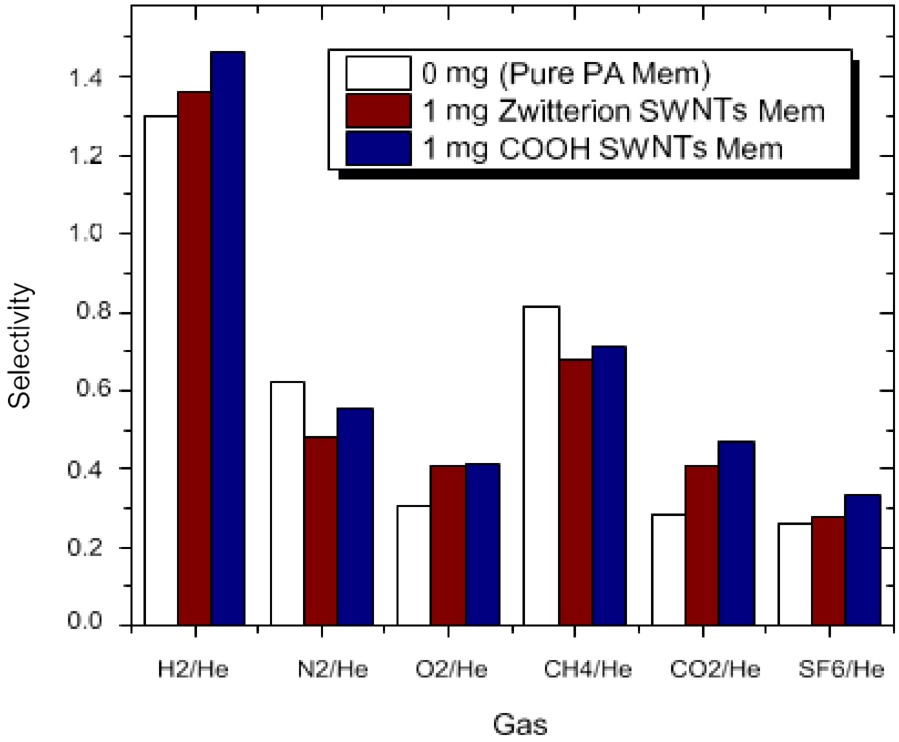

Figure 11.— Selectivities of various light gases through 1 mg SWNT TFN membranes with different functionalizations (zwitterion and carboxylic acid groups).

3.5. Desalination Results

3.5.1. Performance as a Function of CNTs' Concentration

Table 2 show the comparison of different nanocomposite membranes with increasing density of zwitterion-functionalized CNTs. The operating pressures were all identical at 530 psi, and all the membranes have been tested for three consecutive days to examine their stabilities. The feed solution is 1,000 parts per million NaCl in concentration, and the membrane area covered with CNTs is 9.6 square centimeters.

Table 2.—Comparison of Different Nanocomposite Membranes with Increasing Zwitterion-Functionalized CNT Density

	First Day		Second Day		Third Day	
Plain PA	6.7 GFD	97.3%	7.3 GFD	98.1%	6.3 GFD	97.5%
0.25 mg CNTs	14.1 GFD	98.4%	13.3 GFD	98.7%	14.5 GFD	98.5%
0.75 mg CNTs	21.5 GFD	98.6%	20.8 GFD	96.2%	-	-

Note: GFD = gallons per square foot per day

Figure 12 clearly shows that with 0.25 mg of CNTs present in the polyamide membrane, the water flux increased more than twofold, and the salt rejection increased by approximately 1%. When the amount of CNTs increased to 0.75 mg, the flux was three times faster than in the plain polyamide membrane, and the rejection rate was close to 99%.

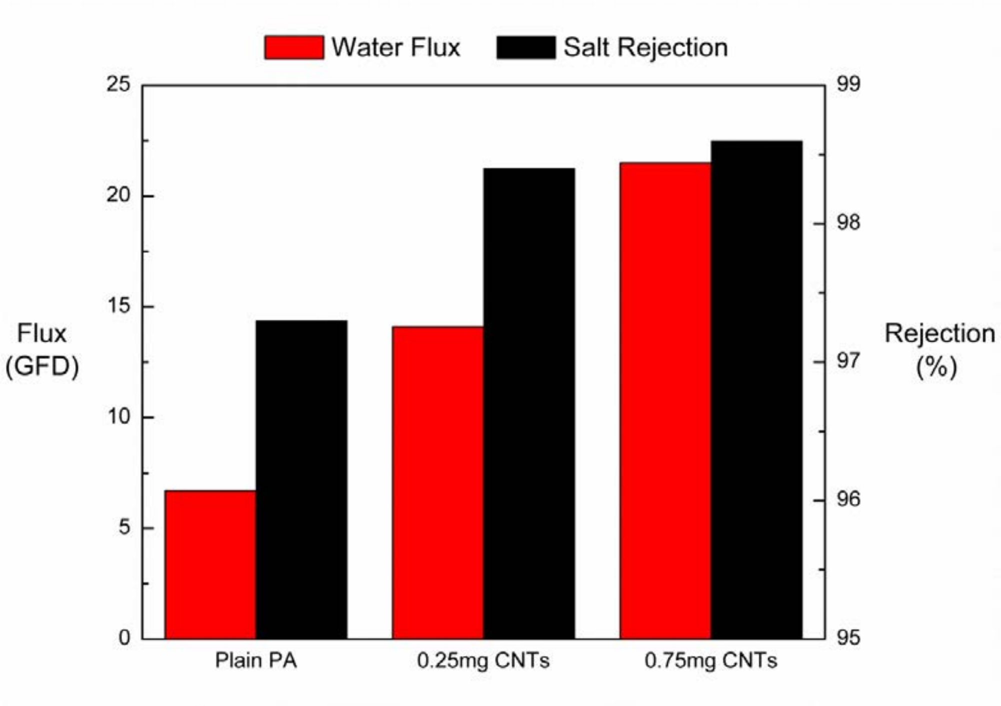

Figure 12.—Water flux and salt rejection (%) as a function of CNT content.

3.5.2. Performance as a Function of Hydraulic Pressure

Figure 13 shows the water flux and the salt rejection as a function of pressure on the membrane with 0.25 mg of CNTs. The overall performance increases as the operating pressure increases. This is consistent with typical RO membrane performance.

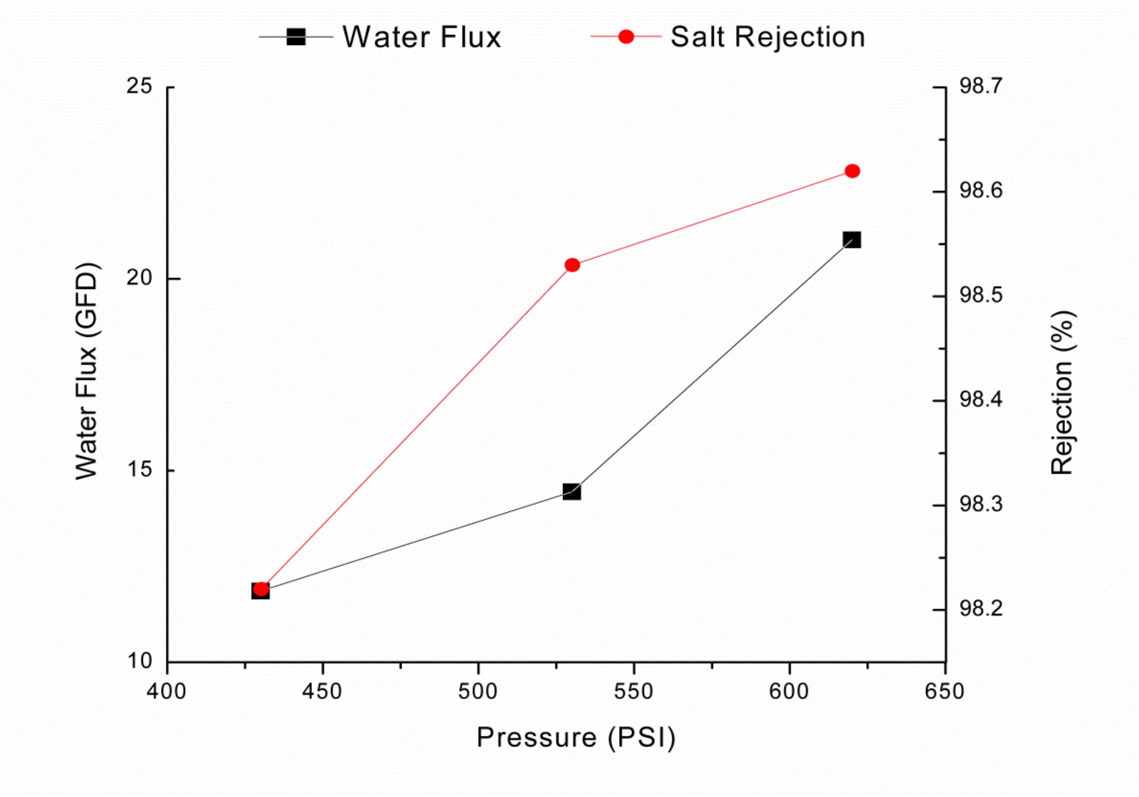

Figure 13.— Water flux and salt rejection as a function of pressure.

Tables 2-4 show the data for all three membranes operating under different pressures.

Table 2.—Plain PA (March 22, 2012)

	First Day		Second Day		Third Day	
425 psi	-	-	4.68 GFD	96.39%	-	-
525 psi	6.70 GFD	97.25%	7.25GFD	98.07%	6.29 GFD	97.49%

Table 3.—0.25 mg-CNT + 0.5 %TMC-PA (March 16, 2012)

	First Day		Second Day		Third Day	
430 psi	-	-	11.86 GFD	98.22%	-	-
530 psi	14.08 GFD	98.35%	13.30 GFD	98.70%	14.45 GFD	98.53%
620 psi	12.73 GFD	98.50%	-	-	21.02 GFD	98.62%

Table 4.—0.75 mg CNT + 0.5%TMC-PA (March 26, 2012)

	First Day		Second Day		Third Day	
350 psi	11.77 GFD	97.32%	8.85 GFD	98.08%	5.37 GFD	95.2 %
425 psi	14.52 GFD	98.09%	13.51 GFD	98.55%	10.93 GFD	91.97%
530 psi	21.53 GFD	98.57%	20.79 GFD	96.21%	-	-

Another membrane with 0.75 mg of CNTs was fabricated and tested for magnesium cation rejection and magnesium ion rejection. As shown in table 5, both showed a high rejection rate.

Table 5.—Reverse Osmosis for 1,000 Parts Per Million Magnesium Sulfate Solution

	Flow Rate	Rejection
310 psi	11.83 GFD	96.18%
410 psi	14.72 GFD	96.09%
500 psi	21.78 GFD	96.41%

4. Conclusions

The zwitterion functionalized CNT membranes demonstrated extremely high transport rates, both for gas and water. Enhancements in gas selectivities were not observed because the CNT pore size was too large to discriminate between gas molecules. On the other hand, when the membranes were employed as desalination membranes, both water flux and salt rejection increased with the addition of the carbon nanotubes. We believe these results occurred because the hydrodynamic radius of hydrated ions is greater than the zwitterion-functionalized CNT pore size and because an electrostatic repulsion exists between the zwitterionic group and the ionic species. We are currently examining the role of the ionic charge on the rejection and flux rates.

5. References

(1) Robeson, L. M. "Correlation of separation factor versus permeability for polymeric membranes", *J. Membrane Sci.* **1991**, *62*, 165--185.

(2) Holt, J. K.; Koy, A.; Huser, T.; Eaglesham, D.; Bakajin, O. "Fabrication of a carbon nanotube-embedded silicon nitride membrane for studies of nanometer- scale mass transport", *Nano Letters* **2004**, *4*, 2245-2250.

(3) Holt, J. K.; Park, H. G.; Wang, Y.; Stadermann, M.; Artyukhin, A. B.; Grigoropoulos, C. P.; Noy, A.; Bakajin, O. "Fast Mass Transport Through Sub-2- Nanometer Carbon Nanotubes", *Science* **2006**, *312*, 1034-1037.

(4) Majumder, M.; Chopra, N.; Andrews, R.; Hinds, B. J. "Nanoscale hydrodynamics - Enhanced flow in carbon nanotubes", *Nature* **2005**, *438*, 44-44.

(5) Majumder, M.; Chopra, N.; Hinds, B. J. "Effect of tip functionalization on transport through vertically oriented carbon nanotube membranes", *J. Am. Chem. Soc.* **2005**, *127*, 9062-9070.

(6) Skoulidas, A. I.; Ackerman, D. M.; Johnson, J. K.; Sholl, D. S. "Rapid Transport of Gases in Carbon Nanotubes", *Phys. Rev. Lett.* **2002**, *89*, 185901.

(7) Skoulidas, A. I.; Sholl, D. S.; Johnson, J. K. "Adsorption and diffusion of carbon dioxide and nitrogen through single-walled carbon nanotube membranes", *J. Chem. Phys.* **2006**, *124*, 054708.

(8) Cheng, G.; Li, G. Z.; Xue, H.; Chen, S. F.; Bryers, J. D.; Jiang, S. Y. "Zwitterionic carboxybetaine polymer surfaces and their resistance to long-term biofilm formation", *Biomaterials* **2009**, *30*, 5234-5240.

(9) Ladd, J.; Zhang, Z.; Chen, S.; Hower, J. C.; Jiang, S. "Zwitterionic polymers exhibiting high resistance to nonspecific protein adsorption from human serum and plasma", *Biomacromolecules* **2008**, *9*, 1357-1361.

(10) Li, G. Z.; Cheng, G.; Xue, H.; Chen, S. F.; Zhang, F. B.; Jiang, S. Y. "Ultra low fouling zwitterionic polymers with a biomimetic adhesive group", *Biomaterials* **2008**, *29*, 4592-4597.

(11) Zhang, Z.; Finlay, J. A.; Wang, L. F.; Gao, Y.; Callow, J. A.; Callow, M. E.; Jiang, S. Y. "Polysulfobetaine-Grafted Surfaces as Environmentally Benign Ultralow Fouling Marine Coatings", *Langmuir* **2009**, *25*, 13516-13521.

(12) Marand, E.; Kim, S. Method for making oriented single-walled carbon nanotube/polymer nano-composite membranes US 2008/0290020A1, 2008; Vol. US 2008/0290020 A1

(13) Ackerman, D. M.; Skoulidas, A. I.; Sholl, D. S.; Johnson, J. K. "Diffusivities of Ar and Ne in Carbon Nanotubes", *Molecular Simulation* **2003**, *29*, 677-684.
(14) Challa, S. R.; Sholl, D. S.; Johnson, J. K. "Light isotope separation in carbon nanotubes through quantum molecular sieving", *Phys. Rev. B* **2001**, *63*, 245419.
(15) Challa, S. R.; Sholl, D. S.; Johnson, J. K. "Adsorption and Separation of Hydrogen Isotopes in Carbon Nanotubes: Multicomponent Grand Canonical Monte Carlo Simulations", *J. Chem. Phys.* **2002**, *116*, 814--824.
(16) Chen, H.; Johnson, J. K.; Sholl, D. S. "Transport Diffusion of Gases Is Rapid In Flexible Carbon Nanotubes", *J. Phys. Chem. B* **2006**, *110*, 1971-1975.
(17) Garberoglio, G.; DeKlavon, M. M.; Johnson, J. K. "Quantum sieving in single walled Carbon nanotubes: effect of interaction potential and rotational- translational coupling", *J. Phys. Chem. B* **2005**, *submitted*.
(18) Gatica, S. M.; Stan, G.; Calbi, M. M.; Johnson, J. K.; Cole, M. W. "Axial phase of quantum fluids in nanotubes", *Journal of Low Temperature Physics* **2000**, *120*, 337-359.
(19) Kuznetsova, A.; Yates, J. J. T.; Simonyan, V. V.; Johnson, J. K.; Huffman, C. B.; Smalley, R. E. "Optimization of Xe Adsorption Kinetics in Single Walled Carbon Nanotubes", *J. Chem. Phys.* **2001**, *115*, 6691--6698.
(20) Matranga, C.; Chen, L.; Smith, M.; Bittner, E.; Johnson, J. K.; Bockrath, B. "Trapped CO_2 in Carbon Nanotube Bundles", *J. Phys. Chem. B* **2003**, *107*, 12930- 12941.
(21) Shi, W.; Johnson, J. K. "Gas adsorption on heterogeneous single-walled carbon nanotube bundles", *Phys. Rev. Lett.* **2003**, *91*, 015504.
(22) Simonyan, V. V.; Johnson, J. K. "Hydrogen storage in carbon nanotubes and graphitic nanofibers", *J. Alloys and Compounds* **2002**, *330-332*, 659--665.
(23) Simonyan, V. V.; Johnson, J. K.; Kuznetsova, A.; Yates, J. J. T. "Molecular simulation of Xe adsorption on single-walled carbon nanotubes", *J. Chem. Phys.* **2001**, *114*, 4180--4185.
(24) Wang, Q.; Challa, S. R.; Sholl, D. S.; Johnson, J. K. "Quantum Sieving in Carbon Nanotubes and Zeolites", *Phys. Rev. Lett.* **1999**, *82*, 956.
(25) Wang, Q. Y.; Johnson, J. K. "Optimization of carbon nanotube arrays for hydrogen adsorption", *J. Phys. Chem. B* **1999**, *103*, 4809--4813.
(26) Holt, J. K. "Carbon Nanotubes and Nanofluidic Transport", *Advanced Materials* **2009**, *21*, 3542-3550.
(27) Skoulidas, A. I.; Sholl, D. S. "Transport Diffusivities of CH_4, CF_4, He, Ne, Ar, Xe, and SF_6 in Silicalite from Atomistic Simulations", *J. Phys. Chem. B* **2002**, *106*, 5058--5067.

(28) Zhu, F.; Tajkhorshid, E.; Schulten, K. "Theory and Simulation of Water Permeation in Aquaporin-1", *Biophysical Journal* **2004**, *86*, 50-57.

(29) Thomas, J. A.; McGaughey, A. J. H. "Water Flow in Carbon Nanotubes: Transition to Subcontinuum Transport", *Physical Review Letters* **2009**, *102*, 184502-184502.

(30) Thomas, J. A.; McGaughey, A. J. H. "Reassessing Fast Water Transport Through Carbon Nanotubes", *Nano Letters* **2008**, *8*, 2788-2793.

(31) Corry, B. "Designing carbon nanotube membranes for efficient water desalination", *Journal of Physical Chemistry B* **2008**, *112*, 1427-1434.

(32) Song, C.; Corry, B. "Intrinsic Ion Selectivity of Narrow Hydrophobic Pores", *J. Phys. Chem. B* **2009**, *113*, 7642-7649.

(33) Joseph, S., and N.R. Aluru, 2008. ”Why are carbon nanotubes fast transporters of water?” *Nano Letters* **2008**, *8*, 452-458.

(34) Hinds, B. J.; N. Chopra, T. Rantell, R. Andrews, V. Gavalas, and L.G. Bachas, 2004. “Aligned multiwalled carbon nanotube membranes,” *Science*, *303*, 62-65.

(35) Rao, A. M.; Eklund, P. C.; Bandow, S.; Thess, A.; Smalley, R. E. "Evidence for charge transfer in doped carbon nanotube bundles from Raman scattering", *Nature* **1997**, *388*, 257--259.

(36) Won, C.Y.; S. Joseph, S., and N.R. Aluru, 2006. “Effect of quantum partial charges on the structure and dynamics of water in single-walled carbon nanotubes,” *Journal of chemical physics*, *125*, 114701-114701.

(37) Suk, M.E., and N.R. Aluru, 2009. “Effect of induced electric field on single-file reverse osmosis,” *Physical Chemistry Chemical Physics*, 8614-8619.

(38) Won, C. Y.; Aluru, N. R. "A chloride ion-selective boron nitride nanotube", *Chemical Physics Letters* **2009**, *478*, 185-190.

(39) Marand, E.; Herrera-Alonso, J.; Suraphathi, A.; Sedlakova, Z. Preparation of functionalized CNTs for UV in-situ polymerization to form CNT/polyacrylic mixed marix membranes; VTIP 10-096 IP disclosure: Virginia Tech, 2010.

(40) Surapathi, A.; Marand, E. Purification effects on the gas sorption in single walled carbon nanotubes. In *NAMS* Charleston, South Carolina, 2009.

(41) Surapathi, A.; Marand, E. Purification effects on the gas sorption in single walled carbon nanotubes. In *239th ACS National Meeting* San Francisco, CA, 2010.

(42) Kim, S.; Pechar, T. W.; Marand, E. "Poly(imide siloxane) and carbon nanotube mixed matrix membranes for gas separation", *Desalination* **2006**, *192*, 210-218.

(43) Kim, S.; Chen, L.; Johnson, J. K.; Marand, E. " Polysulfone and Functionalized Carbon Nanotube Mixed Matrix Membranes for Gas Separation: Theory and Experiment", *J. Membrane Sci.* **2007**, *294*, 147-158.

(44) Kim, S.; Jinschek, J. R.; Chen, H.; Sholl, D. S.; Marand, E. "Scalable fabrication of carbon nanotube/polymer nanocomposite membranes for high flux transport", *Nano Letters.* **2007**, *7*.

(45) Anil Surapathi, Jose M. Herrera – Alonso, Feras Rabie, Steve Martin, Eva Marand “Fabrication and gas transport properties of SWNT/polyacrylic nano- composite membranes”, *Journal of Membrane Science*, 375 (2011) 150-156.